SHAPE EVOLUTION OF STRONTIUM CARBONATE ARCHITECTURES USING NATURAL GUMS AS CRYSTAL GROWTH MODIFIERS

B. Sreedhar,[a,]*, M. Sulochana,[b] Ch. Satya Vani,[c] D. Keerthi Devi,[a] and N. V. Subba Naidu[b]*

Keywords: Keywords: natural gums; screw capped; self assembly; architectures; $SrCO_3$

Strontium carbonate architectures assembled from nanorods are successfully synthesized at room temperature and screw capped method at 100 °C. Our experiments show that the protocol followed for the synthesis of $SrCO_3$ as well as the concentration of various gums used, play an important role in the size and morphology of $SrCO_3$. Here in, we obtained aragonite type nanorod aggregates with unusual morphologies via transformation of metal carbonates at different conditions using natural gums as additives. A rational mechanism based on the oriented self-assembly of $SrCO_3$ nuclei is proposed for the formed architectures. The crystals undergo an interesting morphology changes and have been well characterized by X-ray diffraction (XRD), Scanning Electron Microscopy (SEM), Transmission Electron Microscopy (TEM), Thermogravimetric Analysis (TGA) and Fourier Transform Infrared spectroscopy (FT-IR) techniques. This method is simple, low-cost and environmentally friendly route for the synthesis of $SrCO_3$ architectures with altogether different morphologies.

*Corresponding Authors
Fax: +91-40-27160921
E-Mail: sreedharb@iict.res.in
[a] Inorganic and Physical Chemistry Division, Indian Institute of Chemical Technology (Council of Scientific and Industrial Research), Hyderabad, Andhra Pradesh, 500607, India
[b] Department of Chemistry, Sri Venkateswara University, Tirupati, Andhra Pradesh, 517 502, India Chapters

Introduction

Biomineralization processes to synthesize hierarchical inorganic crystals or hybrid inorganic-organic materials with controlled size and morphology have attracted considerable attention in recent years owing to the importance of such materials in various fields such as medicine, ceramics, catalysis and cosmetics [1]. Fundamental understanding of the formation mechanism and tuning of facile, mild and effective reaction conditions for the synthesis of such materials still remains a great challenge in nanoscience and nanotechnology. Although great progress has been achieved on the synthetic strategies used to date such as co-precipitation, chemical vapor deposition (CVD), hydrothermal route and reverse micelle method, they usually require catalysts, expensive and even toxic templates or surfactants, high temperature, and a series of complicated procedures, thus, suffer from developing tunable protocols to prepare well-defined hierarchical morphology and special architecture forms. Low temperature, surfactant-free, solution-phase chemical fabricating procedure that is environmentally benign and user-friendly still remains a challenge - a struggling task for the synthesis and architecture control of hierarchical nanostructures at room temperature. Use of natural gums – biocompatible and biodegradable materials for bio-inspired morphogenesis strategies is looked as a viable alternative to expensive organic ligands and additives. In continuation of our recent research activities on the use of Gum Acacia (GA) – that is proved to be a very good reducing agent for the reduction of Ag, Pd and Pt, and as a crystal growth modifier for morphological controlled synthesis of $BaCO_3$ and $SrCO_3$, ZnO nanostructures, in the present work we describe our observations of the use of various other gums - Gum Karaya (GK), Gum Kondagagu (GKG), Gum Olibinum (GO) and Gum Tiruman (GT) on the morphology-controlled biomimetic synthesis of $SrCO_3$ architectures.

It is important to select suitable surfactant molecules that act as templates or shape controllers, directing the formation of a structure toward a desired target arrangement – a process of synthesizing inorganic minerals that is controlled by biomolecules or polymers. Biomineralization of $SrCO_3$ complex structures can be easily generated by using natural gums as structure directing agents in ambient and low temperature precipitation experiments in the mineralization process. Strontium carbonate is itself an important raw material in modern electronic industry.[2] Furthermore, strontium carbonate has only one crystal-phase, so it has been widely studied as a model system for bio-crystallization.[3-8] Therefore, controlled synthesis of $SrCO_3$ crystals has attracted much interest. In order to obtain $SrCO_3$ hierarchial superstructures, many additives, as crystal growth modifiers and superstructure-directing reagents, have already been attempted to mimic biomineralization. Strontium carbonate is a very important reagent and has attracted intensive attention because of its interesting additional applications in industry and many other fields: as a constituent of ferrite magnets for small direct current motors, as an additive in the production of glass for color television tubes,[9] production of iridescent and specialty glasses, chemiluminescence sensors, pigments, driers, paints, pyrotechnics,[10-14] strontium metal and other strontium compounds.[10] Very recently, Shi et al. reported the synthesis of $SrCO_3$ nanowires and their catalytic activity to ethanol with reaction temperature.[14] Different fabrication methods for the synthesis of $SrCO_3$ such as self-assembled monolayers,[15-18] ion entrapment method,[7] hydrothermal method,[19,20] microemulsion mediated solvothermal method,[21] homogeneous precipitation by enzyme-catalyzed reaction,[22] biological synthesis using the fungus fusarium oxysporum[23] have been reported. $SrCO_3$ nanostructures with

various morphologies, such as nanowires, nanorods, sphere like and ellipsoid-like particles, were successfully synthesized by a microemulsion-mediated solvothermal method. Du et al[24] reported the synthesis of $SrCO_3$ mesoporous spheres using 1,1,3,3-tetramethylguanidinium lactate as additive. However, there are no reports found in literature on the synthesis of $SrCO_3$ with different sizes and morphologies by employing natural gums, as controlling the morphology- and size-directing reagent.

Natural gums mainly consist of three fractions (1) Highly branched polysaccharide consisting of galactose backbone with linked branches of D-galactose, L-arabinose, L-rhamnose, which terminate in D-glucuronic acid and 4-O-methyl-D-glucuronic acid. (2) Arabinogalactan–protein complex (GAGP–GA glycoprotein) in which arabinogalactan chains is covalently linked to a protein chain through serine and hydroxyproline groups. (3) Glycoprotein having the highest protein content (~50 wt. %). Gum Karaya (GK) is a vegetable gum produced as an exudate by trees of the genus Sterculia and chemically it is an acid polysaccharide. Gum Kondagogu (GKG) is the dried exudates obtained from tree Cochlospermum gossypium which belongs to the family Bixaceae and is a hydrophilic biopolymer. Gum Olibanum (GO) is the dried, gummy exudation obtained from various species of Burseraceae trees and is available in small tears or lumps of white-yellowish or yellow-reddish in colour. Gum Tiruman (GT) or Indian gum is a non-starch polysaccharide. In all these gums, the functional group (-OH) present in arabinose and rhamnose and (-COOH) of glucoronic acids play a crucial role in the growth and formation metal carbonates whereas the proteinaceous core with amino acids stabilize the formed metal carbonates.[25] It not only acts as a stabilizer, [26] but also acts as surfactant and templating agent for which the functional group moieties (–OH, COOH and -NH_2) have been found to play a key role in mimicking the biomineralization process. The crystallization involves the formation of different hierarchical structures like rice grain, doughnut shaped, flower shaped, hexagonal rods and cross shaped which have never been seen before in natural biominerals. Proteins and polysaccharides with complicated patterns of various functional groups in natural gums selectively adsorb on to the metal ion thereby hindering the crystal growth, followed by the mesoscale self-assembly of nanometer-scale building block into hierarchial superstructures.[27-32] The key reaction of CO_2 with Sr^{2+} ions entrapped within the natural gums leads to the growth of beautiful structures of strontianite nanocrystalline, such an aggregated morphology not normally observed using other surfaces as templates.

Recent work carried out in our group showed that natural gum, Gum acacia (GA) could exert a strong influence on external morphology and/or crystalline structure of barium carbonate[33] and strontium carbonate.[34] It was found that different shapes of $BaCO_3$ and $SrCO_3$ particles could be successfully obtained. In order to investigate the availability and functionality of other natural gums - Gum Karaya (GK), Gum Kondagagu (GKG), Gum Olibinum (GO) and Gum Tiruman (GT) on the morphological control of other crystals, further studies needed to be conducted.

In the present investigation, rod-, shuttle-like, peanut, bouquet and sphere-like $SrCO_3$ architectures were achieved by tuning the reaction conditions. This work may provide new insights into the morphological control of $SrCO_3$ particles and the controllable synthesis of other novel inorganic material using natural gums. The objective of the current study was thus to evaluate the ability of different gums to inhibit crystal growth of a model compound comparing the different gums at the same molar ratio in different reaction conditions. However, to the best of our knowledge, controlled synthesis of $SrCO_3$ architectures using natural gums has not been achieved to date.

Experimental Section

Materials and $SrCO_3$ synthesis

Ammonium carbonate $(NH_4)_2CO_3$ and strontium chloride ($SrCl_2$) were of analytical grade and used without further purification. Double distilled water was used in all experiments.In a typical experiment, at room temperature, 0.2662 g (1 mM) of $SrCl_2$ was taken along with different proportions of homogenized natural gums (0.5 % and 1.0 %) in different 25 ml glass beakers. They were dissolved in 20 ml distilled water and the mixed solution was stirred thoroughly with the help of magnetic stirrer. Then $NaHCO_3$ (2 mM; 2 ml) solution is added by continuous stirring and kept for 24 h at room temperature. After 24 h, the crystals formed were filtered washed several times with distilled water and dried at room temperature. A similar solution was prepared and heated to 100 °C and kept at this temperature for a fixed time (5 h) by refluxion in tightly fixed screw cap. After 5 h reaction time the screw cap tubes were allowed to cool to 50 °C and maintained at that temperature for about 15 h before being allowed to cool slowly to ambient temperature over 3 to 4 h. The product was separated from the solution by centrifugation, washed with absolute ethanol three times and dried in vacuum. The sizes and morphologies of the as-synthesized crystals have been well characterized by X-ray diffraction (XRD), Scanning Electron Microscopy (SEM), Transmission Electron Microscopy (TEM), Thermogravimetric analysis (TGA) and Fourier Transform Infrared spectroscopy (FT-IR) techniques.

Characterization

X-ray diffraction measurements of the strontium carbonate architectures were recorded on Rigaku diffractometer (Cu radiation, λ = 0.1546 nm) running at 40 kV and 40 mA (Tokyo, Japan). FT-IR spectra of $SrCO_3$ structures were recorded with a Thermo Nicolet Nexus (Washington, USA) 670 spectrophotometer. The morphology, microstructure and composition of the samples were examined by scanning electron microscopy (FEI Quanta 200 FEG). The crystals were collected on a round cover glass (1.2 cm), washed with deionised water and dried in a desiccator at room temperature. The cover glass was then mounted on a SEM stub and coated with gold for SEM analysis. Thermogravimetric Analysis (TGA) was carried out on a TGA/SDTA Mettler Toledo 851^e system using open alumina crucibles containing samples weighing about 8–10 mg with a linear heating rate of 10 $Kmin^{-1}$ in nitrogen atmosphere (flow rate 30 mL min^{-1}). The morphology, size, and shape distribution of the synthesized $SrCO_3$ nanostructures were observed on TECNAI FE12 TEM instrument operating at 120 kV using SIS imaging software.

The particles were dispersed in methanol and a drop of it was placed on formvar-coated copper grid followed by air drying. The diffraction patterns were recorded at selected area to determine the crystal structure and phases of crystals at 660 mm camera length.

Results and Discussion

Structural characterization of $SrCO_3$ architectures

The phase composition and phase structure of the $SrCO_3$ architectures obtained with various gums - gum karaya (GK), gum kondagagu (GKG), gum olibinum (GO) and gum tiruman (GT) at two different gum concentrations (0.5 % and 1.0 %) in screw capped and room temperature methods were examined by XRD. Since all the different shapes have same composition, XRD patterns of the as-synthesized materials without gum and with 1 % gum concentration of the various gums at 100 ^{o}C by screw capped method are only shown in Figure 1.

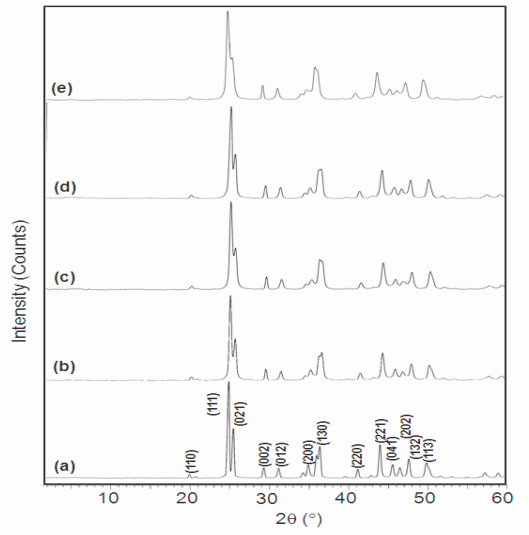

Figure 1. XRD patterns of as synthesized $SrCO_3$ hierarchical architectures obtained without gum (a), with 1% GK (b), 1 % GKG (c), 1 % GO (d), and 1 % GT (e) in pressure vial at 100 °C for 5 h.

As strontium carbonate is a single-phase crystal, it could be seen that XRD patterns of $SrCO_3$ prepared with different gums have the same diffraction pattern and all the peaks could be perfectly indexed to a pure orthorhombic structure of strontium carbonate (space group Pmcn {62}) of $SrCO_3$ with lattice constants *a* = 5.107 Å, b = 8.414 Å, and c = 6.029 Å (JCPDS card no.05-418) and no characteristic peaks from other impurities have been detected indicating that the as-synthesized products have high phase purity. The XRD patterns of $SrCO_3$ presented in Figure. 1 exhibit peaks characteristic of scattering angles (2θ) at 20.3, 25.1, 25.8, 29.5, 31.2, 35.1, 36.5, 41.2, 44.0, 45.5, 46.3, 47.7 and 50.1 corresponding to the following diffraction peaks with (*hkl*) indices (110), (111), (021), (002), (012), (200), (130), (220), (221), (041), (202), (132), and (113) crystallographic planes, respectively similar to pure orthorhombic strontionite [JCPDS-05-418]. It may also be seen that the peak (111) is the strongest, suggesting that $SrCO_3$ crystals obtained at both room temperature and screw capped methods, grow mainly along with the (111) phase.The strong and sharp diffraction peaks in Figure 1 indicate that the as obtained $SrCO_3$ hierarchical architectures are principally crystalline. The absence of some diffraction peaks in Figure 1b-e, when compared to the XRD pattern of $SrCO_3$ crystals obtained without gum (Figure 1a) is due the presence of gum on the crystal faces, resulting into the formation of an organic–inorganic hybrid material that is in consonance with the observations in TGA analysis.

Effect of additives on the morphology and size of $SrCO_3$

The SEM micrographs at both lower and higher molar ratio (0.5 % and 1 %) of different natural gums in ambient and screw capped method have been characterized. Figures 2 and 4 show low magnification SEM micrographs of $SrCO_3$ particles obtained from aqueous solution in the absence and presence of different gums namely, gum karaya (GK), gum kondagagu (GKG), gum olibinum (GO), gum tiruman (GT) synthesized at room temperature and screw capped method at 100 °C. As can be seen from Fig. 2, in the absence of gum, the as-obtained particles appeared bundle-like dendrimers consisting of many small $SrCO_3$ needles aligned radially towards both ends. Flower-like and bouquet like morphologies of $SrCO_3$ nanostructures are seen with gum karaya (GK) and gum kondagagu (GKG). Peanut like morphologies are observed commonly in both gum olibinum (GO) and gum tiruman (GT). At higher magnification (Figure 3 and Figure 5) nanocrystals self assembled into interesting morphologies can be clearly seen.

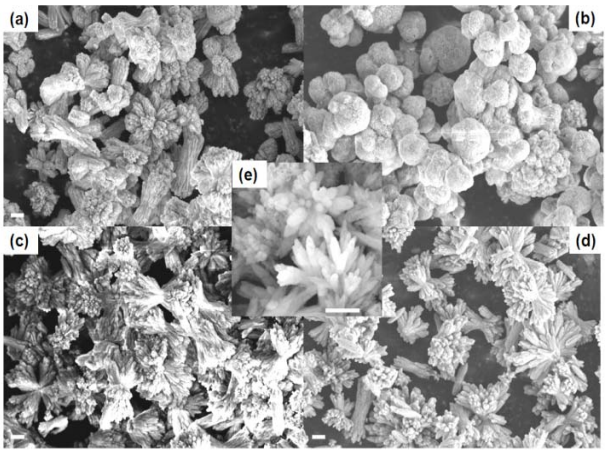

Figure 2. Low magnification SEM images of as synthesized $SrCO_3$ hierarchical architectures obtained with 1 % GK (a), 1 % GKG (b), 1 % GO (c) , with 1 % GT (d), and without gum (e) at room temperature. Scale bar measures 1 µm.

To know the influence of concentration of the various gums on the morphology and size of the products, separate experiments were carried out using 0.5 and 1.0 % gums. Except for a small decrease in the size of the nanostructures, no significant change in the morphology of the synthesized $SrCO_3$ architectures were identified by changing the concentration of the various gums. This behavior can be attributed due to the effective passivation of the surfaces and suppression of the growth of the nanoparticles through strong interactions with the particles via their main functional molecular groups of gums namely, hydroxyl groups and carboxylic groups. Further observation shows that there exist many fragments ruptured at the middle parts

of the bundles. Therefore, it could be inferred that the middle parts of the bundles are more fragile than their radial branches. When 0.5 % of the various gums were added into the reaction mixture, the morphology of $SrCO_3$ particles formed showed a significant difference, when compared to the above mentioned bundle like dendrimers formed in the absence of gum.

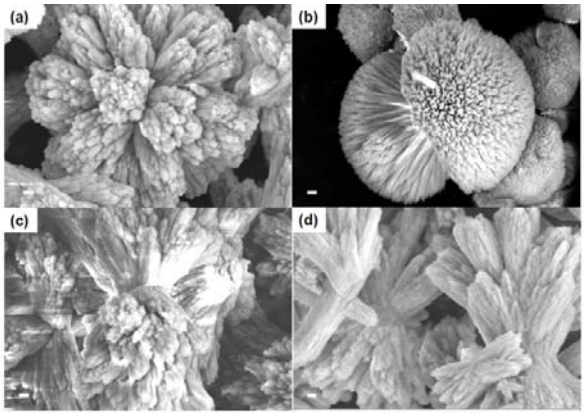

Figure 3. High magnification SEM images of as synthesized $SrCO_3$ hierarchical architectures obtained with 1 % GK (a), 1 % GKG (b), 1 % GO (c) , and 1 % GT (d) at room temperature. Scale bar measures 200 nm.

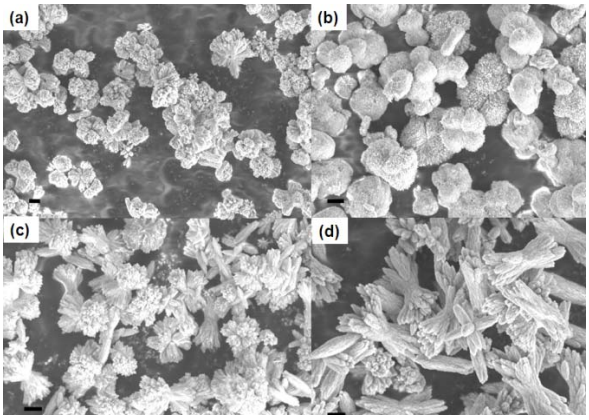

Figure 4. Low magnification SEM images of as synthesized $SrCO_3$ hierarchical architectures obtained with 1 % GK (a), 1 % GKG (b), 1 % GO (c) , and 1 % GT (d) in pressure vial for 5 h. Scale bar measure 1 µm.

The morphology of as synthesized particles with the various gums are more homogenous whatever may be the shape or size they are appearing in and the flower like particles with branches consist of self assembled nanoparticles. Further, on increasing the concentration of the gum (1.0 %), the shape of the formed architectures though remained same showed a decrease in size and depended on the gum used for the synthesis. Significant decrease in size was observed with GK that can be attributed due to the selective oriented adsorption of GK on crystal faces along the growth direction of the needle like branches and due to steric inhibition limits the growth of the needles. At higher concentration of GK (1.0 %), the ends of the dumbbell ends tend to become large and the part that undergoes quenching self-assemble to form of flower like structure with nanocrystals. But in GKG, when the concentration is raised to 1.0 %, like shape with nanocrystals were obtained. As can be seen in Figure 3b, the formation of the nanostructure starts from the centre and then the crystals start to assemble on either direction with the ends of the bouquet having a larger semi circular morphology. In the case of both GO and GT, the structures formed appear more or less similar in morphology - peanut like structures consisting of aggregated nanocrystals. These peanut like structures appear to be overlapping to form flower like structures with GT (Figure 3d).

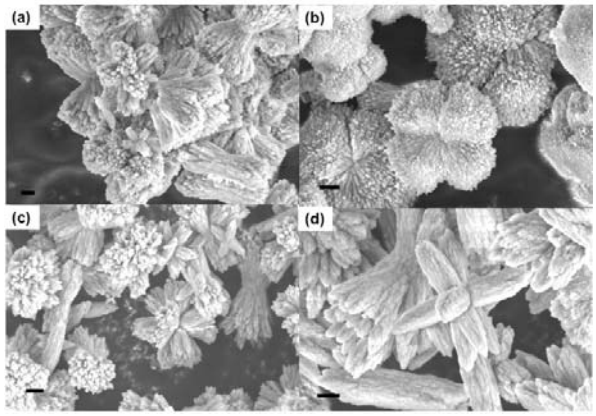

Figure 5. High magnification SEM images of as synthesized $SrCO_3$ hierarchical architectures obtained with 1 % GK (a), 1 % GKG (b), 1 % GO (c) , and 1 % GT (d) in pressure vial for 5 h. Scale bar measure 500 nm.

The morphology and structure of the as-formed $SrCO_3$ architectures was further confirmed by TEM and the images are shown in Figure 6. As can be seen in Figure 6 individual architectures consisting of nanorods with perfect bouquet, flower like and pea nut like assembly, in accordance to the observations from SEM.

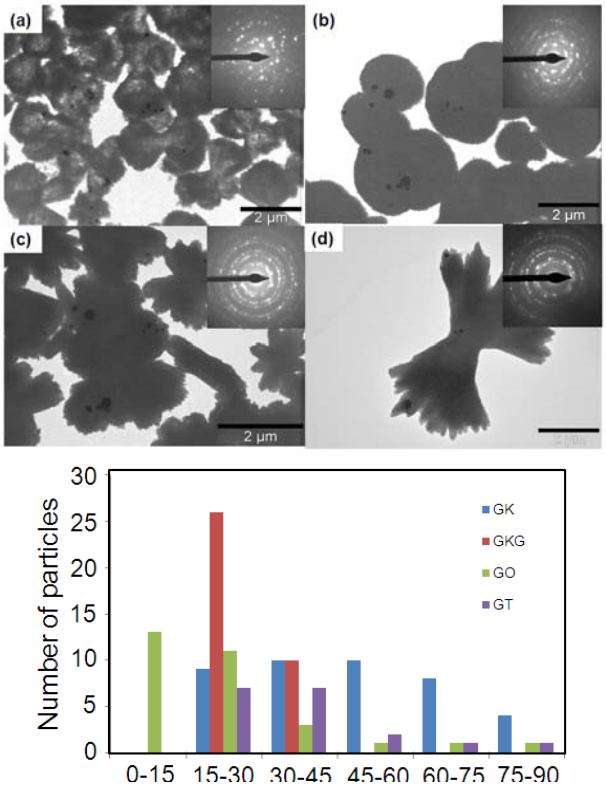

Figure 6. TEM images of as synthesized $SrCO_3$ hierarchical architectures obtained with 1 % GK (a), 1 % GKG (b), 1 % GO (c), 1 % GT (d) gums in pressure vial for 5h with the respective SAED pattern (inset) and particle size distribution (e).

As we have not observed $SrCO_3$ as discrete nanorods even at room temperature or in screw capped reaction of 5 h, it clearly indicates that these architectures are actually integrated and are not just aggregations of nanorods into different shapes. The size of the as obtained nanoparticles in screw capped method show a significant dependence on the gums used i.e., for GK 17 - 78 nm, GKG 20 - 38 nm, GO 9 - 58 nm and GT 25 - 57 nm as shown in the particles size distribution figure in Figure 6e. The corresponding selected area electron diffraction patterns for all the as-synthesized $SrCO_3$ from various gums show clear diffraction spots, reiterating the crystalline nature of the formed nanostructures. Both the XRD and SAED analysis indicate that the anisotropic growth of these architectures is along (111) direction.

FTIR analysis

To identify the growth mechanism and the effect of the different gums on $SrCO_3$ architectures, the samples were analysed by FT-IR spectroscopy.

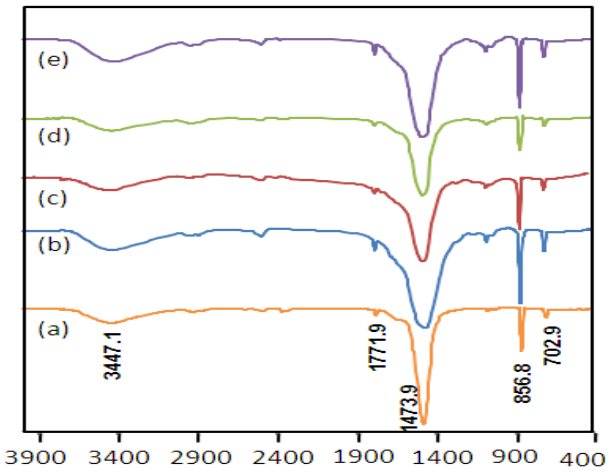

Figure 7. FT-IR spectra of as synthesized $SrCO_3$ hierarchical architectures obtained without gum (a), with 1 % GK (b), 1 % GKG (c), 1 % GO (d), and 1 % GT(e) at room temperature.

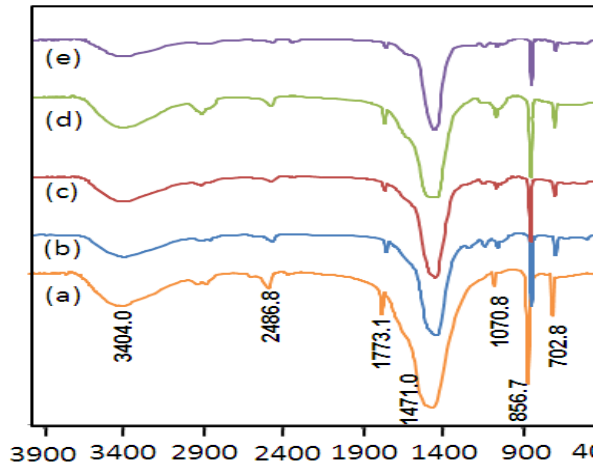

Figure 8. FT-IR spectra of as synthesized $SrCO_3$ hierarchical architectures obtained without gum (a), with 1 % GK (b),1 % GKG (c), 1 % GO (d), and 1 % GT(e) in pressure vial at 100 °C for 5 h.

The sharp peaks at 856.8, 702.9 cm^{-1} (Figure 7), 856.7, 702.8 cm^{-1} (Figure 8) are due to the in-plane and out-plane bending of CO_3^{2-} group. The IR bands at 1473.9 and 1471.0 cm^{-1} (Figure 7 , 8) correspond to the asymmetric stretching mode of C-O bond while the weak band at 1070 cm^{-1} is attributed to the symmetric C-O stretching vibration. The band at 3447 and 3404 cm^{-1} can be attributed to OH stretching vibration due to hydrogen bonding and/or N-H stretching of the $–NH_2$ group from the functional groups present in additives. The characterized peaks at 1070, 856, 1473 and 702 cm^{-1} of $SrCO_3$ crystal correspond to the ν_1, ν_2, ν_3 and ν_4 vibration modes, respectively and at 1771.9 and 1773.1 cm^{-1} belongs to the C=O stretching vibration of carboxyl groups.

The FTIR results indicate that all the gums used in this study get adsorbed on the crystal faces during the mineralization process that directs the self-assembling of nanocrystals resulting in interesting architectures and form organic-inorganic hybrid materials.

Thermogravimetric studies

Thermogravimetric analysis helps us to understand the decomposition steps more precisely as we can know the evolved gas fragments as a function of temperature or time. As representative systems, the TG/DTG thermograms of $SrCO_3$ synthesized with GK, GKG, GO and GT at 100 °C in screw capped reaction are shown in Figure 9a, b, c, d, respectively.

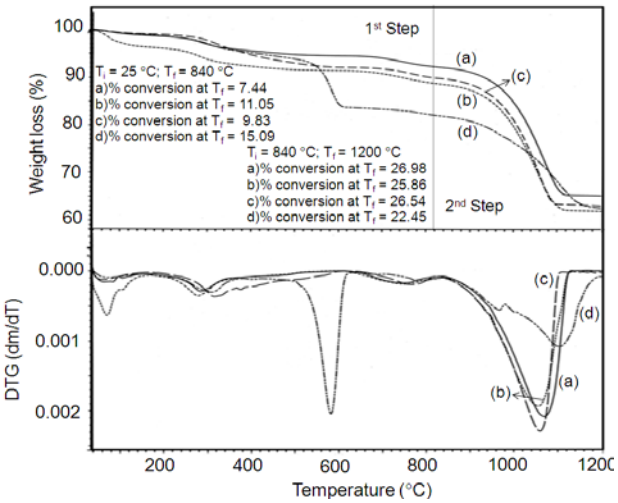

Figure 9. TGA-DTG thermograms of as-synthesized $SrCO_3$ hierarchical architectures obtained with 1 % GK (a), 1 % GKG(b), 1 % GO (c), and 1 % GT (d) in pressure vial at 100 °C for 5 h.

TGA profile of $SrCO_3$ structures synthesized without gum[37] shows a single step decomposition in the range 850–1050 °C. The corresponding mass loss was quite similar to the theoretical value of the mass loss of the above decomposition (29.81 %) and almost the same with that occurred for the thermal decomposition of the high pure $SrCO_3$ phase between 900–1150 °C.[35] Figure 8 represents the TG-DTG thermograms of $SrCO_3$ with various gums. The first step in the temperature range between 25–840 °C is due to the decomposition of the various gums in the as-synthesized $SrCO_3$ nanostructures. Similar decomposition

profile was observed in $SrCO_3$ nanocrystallites synthesized using GA that was ascribed due to the evolution of CO_2 (mass fragment 44 a.m.u, from the decomposition of –COOH functional groups in GA) from GA component in the inorganic and organic hybrid $SrCO_3$ nanocrystallites.[37] The second step in the temperature range 840-1200 °C can be attributed mainly due to the decomposition of $SrCO_3$ nanocrystallites into SrO and CO_2. The corresponding mass losses were found to be 26.98 % (GK), 25.86 % (GKG) 26.54 % (GO), and 22.45 % (GT) that correspond to 29.1 %, 29.0 %, 29.4 %, and 26.4 % respectively of CO_2 from the $SrCO_3$ nanostructures and that are close to the theoretical value of the mass loss ~ 30 % of the high pure $SrCO_3$ phase between 900–1150 °C. The decrease in the amount of decomposition for the $SrCO_3$ nanostructures when GT is used as the additive may be due to the incomplete decomposition of the sample till 1200 °C. The temperature of maximum decomposition of $SrCO_3$ is found to be 1070, 1052, 1060 and 1105 °C for GK, GKG, GO, and GT, respectively. This variation in the temperature can be ascribed to the size effect of the nanoparticles existing within the nanocrystallites of the formed inorganic-organic hybrid materials.

Conclusions

In summary, uniform hierarchical $SrCO_3$ architectures in the form of bouquet, peanut, and flower like morphologies were efficiently obtained by using natural gums as crystal growth modifiers at room temperature and screw capped methods at 100 °C which are confirmed by SEM and TEM micrographs. The crystalline nature and spectral features of strontium carbonate is confirmed by XRD and SAED pattern and FTIR, respectively. TGA study confirms that the as synthesized $SrCO_3$ nanocrystallites using various gums are having both inorganic and organic components resulting into the formation of inorganic-organic hybrid materials. It can be concluded that the whole growth process of $SrCO_3$ was affected by the additive and the reaction conditions. This simple protocol emphasizes that it is possible to fabricate the different morphologies and sizes of $SrCO_3$ particles with self assembly hierarchical architectures assisted by natural gums as additives and can be used in many potential applications.

Acknowledgements

MS and NVSN thank DIICT for giving opportunity to carry out a part of the present work at CSIR-IICT, Hyderabad, India.

References

[1]Braun, P. V., Osenar, P., and Stupp, S. I., *Nature* **1996**, *380*, 325.

[2]Omata, K., Nukui, N., Hottai, T., Showa, Y., and Yamada, M., *Catal. Commun.,* **2004**, *5(12),* 755.

[3]Kuther, J., Nells, G., Seshadri, R., Schaub, M., Butt, H. J., and Tremel, W.,*Chem. Eur. J.* **1998,** *4(9)*,1834.

[4]Kuther, J., Seshadri, R., Nells, G., Assenmacher, W.. Butt, H. J., Mader, W., and Tremel, W., *Chem. Mater.,* **1999**, *11(5)*,1317.

[5]Kuther, J., Bartz, M., Seshadri, R., Vaughan, G. B. M., and Tremel, W. J., *Mater. Chem*., **2001**, *11(2)*, 503.

[6] Sastry, M., Kumar, A., Damle, C., Sainkar, S. R., Bhagwat, M., and Ramaswamy, V., *Cryst. Eng. Commun*., **2001**, *3(21)*, 81.

[7] Rautaray, D., Sainkar, S. R., and Sastry, M., *Langmuir,* **2003**, *19(3)*, 888.

[8]Qi, L., Xi, K., and Ma, J., *Acta Chimica Sinica*, **2003**, 61(*1)*, 126.

[9]Bastow,T. J., *Chem. Phys. Lett.* **2002**, *354(1-2)*, 156–159.

[10]Zeller, A. F., *Chem. Tech*., **1981**, *19*, 762.

[11]Griffiths, J., *Ind. Miner.,* **1985**, *218,* 21.

[12]Erdemoglu, M., and Canbazoglu, M., *Hydrometallurgy*, **1998**, *49(1-2)*,135.

[13]Owusu, G., and Litz, J. E., *Hydrometallurgy*, **2000**, *57(1)*, 23.

[14]Shi, J. J., Li, J. J. , Zhu, Y. F., Wei, F., and Zhang, X. R., *Anal. Chim. Acta*, **2002**, *466(1)*, 69.

[15]Aizenberg, J., Black, A.J., and Whitesides, G. M., *J. Am. Chem. Soc.*, **1999**, *121(18)*, 4500.

[16]Küther, J., Bartz, M., Seshadri, R., Vaughanc, G. B. M., and Tremela, W., *J. Mater. Chem.*, **2001,** *11(2)*, 503.

[17]Kuther, J., Nelles, G., Seshadri, R., Schaub, M., Butt, H. J. , and Tremel, W., *Chem. Eur. J.,* **1998**, *4(9)*, 1834.

[18]Kuther, J., Seshadri, R., and Tremel, W., *Angew. Chem., Int. Ed.*, **1998**, *37(21),* 3044.

[19]Li, S.Z., Zhang, H., Xu, J., Yang, D.R., *Mater. Lett*., **2005**, *59*, 420.

[20]Huang, Q., Gao, L., Cai, Y., and Aldinger, F., *Chem. Lett*., **2004**, *33(3)*, 290.

[21]Cao, M.H., Wu, X.L. , He, X.Y., and Hu, C.W., *Langmuir*, **2005,** *21(13)*, 6093.

[22]Sondi, I., and Matijevic, E., *Chem. Mater*., **2003**, *15(6)*,1322.

[23]Rautaray, D., Sanyal, A., Adyanthaya, S.D., Ahmad, A., and Sastry, M., *Langmuir,* **2004**, *20(16)*, 6827.

[24]Du, J.M., Liu, Z.M., Li, Z.H., Han, B.X., Huang, Y., and Zhang, J.L., *Micro. Meso. Mater.,* **2005,** *83(1-3)*,145.

[25]Devi, D. K., Pratap, S. V., Haritha, R., Sivudu, K. S, Radhika, P., and Sreedhar, B., *J. Appl. Polym. Sci.*, **2011**,*121(3)*,1765.

[26]Sreedhar, B., Reddy, P. S., and Devi, D. K., *J. Org. Chem.*, **2009**, *74(22)*, 8806.

[27]Yu, S. H., and Colfen, H., *J. Mater. Chem*., **2004**, *14(14)*, 2124.

[28]Colfen, H., and Antonietti, M., *Langmuir*, **1998**, *14(3)*, 582.

[29]Sommerdijk, N. A. J. M., *Chem. Rev.* **2008**, *108(11)*, 4499.

[30]Colfen, H., *Macromol. Rapid Commun.,* **2001**, *22(4)*, 219.

[31]Qi, L. M., Colfen, H., Antonietti, M., Li, M., Hopwood, J. D., Ashley, A. J., and Mann, S., *Chem. Eur. J.*, **2001**, *7(16)*, 3526.

[32]Qi, L. M. , Colfen, H. , Antonietti, M., *Angew. Chem. Int. Ed.*, **2000**, *39(3)*, 604.

[33]Sreedhar, B., Satya Vani, Ch., Keerthi Devi, D., Sreeram, V., Basaveswara Rao, M. V., Rambabu, C., *Am. J. Mater. Sci.* **2012,** *2(5)*, 142.

[34]Sreedhar, B., Satya Vani, Ch., Keerthi Devi, D., and Basaveswara Rao, M. V., Rambabu, C., and Saratchandra Babu, M., *Cryst. Res. Technol.*, 2011, *46(5)*, 485.

[35]Liu, X. , Peng, X., Xie, W., Wei,Q., *Chin. J. Mater. Res*., **2005,** *19*, 287.

Received: 24.12.2014.
Accepted: 20.01.2014.